

# PERFORMANCE CHARACTERIZATION OF THE SUNPOWER CRYOCOOLER

G.T. Smedley, R.G. Ross, Jr.  
Jet Propulsion Laboratory  
1540 E. California Blvd., Pasadena, CA 91109

D. M. Berchowitz  
Sunpower Inc.  
Athens, GA 30601

## ABSTRACT

The Sunpower 140K cryocooler is an integral in-line single compressor/single displacer configuration that features the use of low friction gas bearings on all running surfaces. The design is very compact, simple, and light-weight. This type of cryocooler was originally intended for use in the electronics industry. The original machine provided 35 watts of cooling at 223 K at a heatsink temperature of 45°C with 65 watts of input power. The 140 K cooler, characterized by JPL, is a modified version of the original cooler and achieves 4 to 8 watts of cooling over the temperature range 120 K to 140 K with less than 70 watts of input power.

The Sunpower 140K cryocooler was characterized by JPL in a number of performance areas including thermal, vibration, resonance, EMI, and off-state parasitic. The results of these measurements are presented; where possible, the measurements are compared with calculated performance curves.

## INTRODUCTION

The Sunpower 140K cryocooler was characterized by JPL in a number of performance areas including thermal, vibration, resonance, EMI, and off-state parasitics [1]. The results of these performance measurements are summarized in this paper and comparisons are made to calculated performance curves provided by Sunpower. This cryocooler is a compact, light-weight, in-line cooler that utilizes a single compressor and displacer. The compressor is driven at a frequency of 60 Hz by a linear permanent-magnet motor, while the displacer is passively driven by the compressor pressure wave. The displacer piston is centered using a mechanical spring and the compressor piston is centered using a magnetic spring. Helium gas is used as the working fluid and cooling is achieved according to the Stirling cycle. Due to the free piston design, gas bearings are used to provide contact-free motion. Sunpower created the 140K cryocooler by modifying a Sunpower Minicooler, capable of lifting ~35 watts at 220 K with a 45°C heat rejection temperature, that was originally developed for electronic cooling. The modifications were limited to optimization of the regenerator to achieve lower temperatures, increasing the coldfinger length to reduce conduction losses, and removal of the original heat rejection fins intended for convective cooling. A schematic of the resulting prototype cooler is shown in Fig. 1.

The Sunpower coolers have no built-in instrumentation for monitoring compressor or displacer stroke, except during development/testing at Sunpower. Therefore, characterization of the cooler was performed using constant input voltage. In general, thermal and vibration performance were measured with 5.3, 8.0, and 10.0 Vrms input to look at the sensitivity of the performance to the drive voltage. The resonance measurements were conducted while powering the cooler with a

current-mode amplifier and 1 μM measurements were made while the cooler was operated at 10.0 Vrms input.

## PERFORMANCE ANALYSIS

In general, a combination of oscillatory flow models, non-steady heat transfer, and empirical results are used to predict the performance of a particular cooler. Occasionally, fine tuning of the performance may be facilitated by computer simulation of the flow conditions and heat transfer within the cooler. However, the use of these simulation techniques is exceedingly slow, even on supercomputers, and they do not lend themselves easily to design optimization. This is partially due to the fact that these simulations are essentially complex numerical experiments that are difficult to interpret when trying to gain a clear physical understanding of the entire dynamic system.

Despite the fact that the flow and heat transfer phenomena within the cooler are extremely complex, the response of the entire cooler system is remarkably linear. In its simplest form, the cooler may be described as a tuned mechanical oscillator where the resonances of the displacer and the compressor are set to obtain the optimum phase angles for both thermodynamic and electrical performance. Therefore, linearization of the governing equations [2, 3, 4] results in a minimal loss of accuracy and allows a simple physical interpretation of the interacting thermodynamics and mechanical dynamics. This simplicity is essential in enhancing the understanding of test data during the development phase of the cooler and quickly leads to convergence in the design optimization process.

In the following presentation of the refrigeration performance data, the linearized model described in [2, 3, 4] is used to predict the performance at the measured conditions so that a comparison between the calculated results and the experimental results can be made. The linear model makes use of the physical characteristics of the 40K cooler but is not tuned to match any of the thermal performance points.

An outline of the use of the model is described here, for a more detailed treatment of the model specifics, refer to the references. The model is set up to use the cold tip temperature  $T_c$ , the heatsink temperature  $T_h$ , and the piston stroke  $X_p$  as its fundamental inputs; however, the stroke information was not available from the measurements (due to the lack of stroke instrumentation). The fundamental results of the model are the lifted heat  $Q_l$  and the input power to the thermodynamic cycle  $P_{cycle}$ . In order to perform time calculations, it was therefore necessary to determine the piston stroke that yielded the measured input power at each of the operating conditions. The experiments were conducted at constant input voltage while the input current  $I_{motor}$  and the input power  $P_{motor}$  to the motor were measured. The AC resistance of the motor coil was 0.168 ohms. A permanent magnet is used to center the compressor piston and to provide additional spring force, which leads to an additional power loss  $P_{magloss}$ . Therefore, the power to the cycle is expressed as:

$$P_{cycle} = P_{motor} - (I_{motor})^2 R_{coil} - P_{magloss}$$

The power loss (due to the presence of the magnet) was measured at Sunpower by driving this cooler motor with another motor. The input power to the well characterized driving motor was taken as the magnetic loss and was attributed primarily to the presence of the permanent magnet. A plot of this power loss is shown in Fig. 3 as a function of the piston stroke. The stroke  $X_p$  must be known before the amount of magnetic loss  $P_{magloss}$  can be determined.

The model was supplied with the measured temperatures  $T_c$  and  $T_t$ , along with a piston stroke that was estimated from the measured input power. The model yielded a cycle input power  $P_{cycle}$  and a heat lift  $l$  for those operating conditions. This new cycle power  $P_{cycle}$  plus the magnetic loss  $P_{magloss}$ , determined from the chosen stroke using Fig. 3, was compared to the measured input power ( $P_{motor} - (I_{motor})^2 R_{coil}$ ). If a difference was found, the stroke was modified. This new stroke along with  $T_c$  and  $T_t$  was run through the model again to produce a new cycle power  $P_{cycle}$ . This process was repeated until the determined  $P_{cycle} + P_{magloss}$  was equal to the measured input power, meaning that the correct stroke for the measured input power had been found. The final heat lift  $l$  and stroke  $X_p$  were the results of the linearized model that were determined for the measured input power and the measured temperatures  $T_c$  and  $T_t$ .

## REFRIGERATION PERFORMANCE

The Sunpower 140K cooler has excellent thermal efficiency and provides nearly 7 watts of cooling at 140 K with just over 4(J watts of input power. The cooler refrigerates - 100 gm of copper from ambient temperature to 134 K in 30 minutes at a drive voltage of 8.0 Vrms with no apparent anomalies. The cooler is extremely compact and light weight for a cooler of its thermal capacity. Although the efficiency of the drive motor is good (75 to 80%) there may be room for further improvement, as the power factor is less than 0.9 at cryogenic operating conditions.

As mentioned above, the 140K cooler resulted from the modification of a Minicooler that was not designed to attain such low temperatures. The motor in the 140K cooler is identical to the one used in the Minicooler; however, it must be operated at higher powers than it was designed for in order to achieve these lower temperatures. In addition, due to the increased internal volume and redesigned regenerator, the resonant frequency of the piston is lower at room temperature than it was in the original Minicooler. This non-optimal resonance results in a significant reduction in the power factor as the cold tip temperature decreases. The 140K cooler was not tuned in the way that a completely new design would normally be tuned.

**Test Apparatus** The refrigeration performance measurements were conducted in the JPL thermal-vacuum test facility that is used to simulate conditions in space and to provide a highly stable thermal test environment; the high level of environmental stability allows accurate repeatable measurements to illuminate subtle and important performance sensitivities. The cooler was attached to a copper flange, thermally isolated from the vacuum housing, to allow accurate control of the heatsink temperature using a fluid-loop heat exchanger. The cold tip was outfitted with a cryo-diode to measure the cold tip temperature and a metal film resistor was used to apply a heatload. The cold tip was wrapped in several layers of aluminized Kapton ML1 to reduce any parasitic radiation heat load to negligible levels and the vacuum was maintained below  $10^{-5}$  torr to avoid gaseous conduction effects.

The cooler was driven using a low distortion audio amplifier with a sinusoidal voltage waveform. The power to the cooler was monitored using a high-quality true-RMS power meter. Because drive-cable ohmic losses are read by the power meters, cable ohmic losses were also separately measured and were subtracted out in the final power data that are reported in the figures.

**Motor Efficiency** Fig. 2 shows the measured motor efficiency as a function of the input power at various drive voltages and heatsink temperatures; each data set was obtained by increasing the cold tip heat load with the no-load point having the lowest motor efficiency in each data set. Note that the motor efficiency falls off at the higher input power levels that are required to reach the lowest temperatures. At higher input power, the input power increased as the heatload was

increased; while at lower input powers, the input power remained nearly constant or decreased as the heat load was increased. It is clear from this plot that this cooler prefers to operate at higher coldtip temperatures where the motor efficiency is greater; it is also clear that there is room for improved low temperature performance by utilizing a motor with higher efficiency at higher input powers. If this motor had an efficiency of 90%, the power lost in the coil would decrease by a factor of two; the recovered power could be converted to useful cooling work. For example, a motor that is 80% efficient requires 70 watts of input power to do 56 watts of work, whereas a motor with an efficiency of 90% would require only 62 watts of input power to do the same amount of work. In addition, by tuning the cooler so that the piston and displacer achieve larger strokes for a given input power, more gain in lifted heat would be achieved for a given input power.

**Thermal Performance** The performance of the 140K cooler was calculated at each of the experimental test points using the linear model; for the sake of brevity only the results obtained at 20°C heatsink temperature will be discussed. Fig. 4 maps the thermal performance of the Sunpower 140K cooler with respect to five key parameters: input power, cold tip load, specific power, cold tip temperature and compressor input voltage. Both the measured results and the calculated results are presented on the same plot for comparison. Recall that it was not possible to measure the compressor stroke, since there is no available stroke-length instrumentation. For this plot the heatsink temperature is fixed at 20°C. Three horizontal constant-voltage load lines are presented covering compressor input voltages from 5.3 V<sub>rms</sub> to 10.7 V<sub>rms</sub>. **Notice** that the input power is strongly dependent on the compressor input voltage and is only weakly determined by the coldtip load and coldtip temperature; the calculated results reflect the same basic phenomena. This is typical of small Stirling-cycle cryocoolers. The predicted power and the measured power are the same, since this was one of the inputs to the model. Notice also that the isotherm lines (lines of constant coldtip temperature) are less steeply sloped than the constant specific power lines; thus the refrigerator efficiency is greater at higher input voltage. The isotherms determined from the calculated performance data compare very well with the isotherms determined from the measured performance data between the 5.3 and 8.0 V<sub>rms</sub> curves. Between the 8.0 and 10.7 V<sub>rms</sub> curves, the isotherms from the calculated data are somewhat more optimistic than the isotherms from the measured performance; this is due to predicted loads being larger than actual loads for a given coldtip temperature.

Another view of the comparison of this data to the calculated performance is shown in Fig. 5 where the cold tip heatload (Lift) is plotted against the coldtip temperature. Notice once again, that the calculated results match the measured ones very well for the 5.3 and 8.0 V<sub>rms</sub> data; whereas the calculated results are higher than the measured ones for the 10.7 V<sub>rms</sub> data. At a drive voltage of 10.7 V<sub>rms</sub>, the input power to the cooler is quite high and the efficiency of the motor has degraded, it is impressive that the linearized model dots so well despite these extremes. Note, that unlike load curves from most cryocoolers, these load curves show little sign of bending over in a concave down type of shape. These data appear to be following a concave upward path; in fact, least-squares quadratic curve fits yield positive coefficients on the squared term. This phenomenon is discussed below in the Load Curve Concavity subsection.

**% Carnot COP** These calculated performance data can also be used to determine the %Carnot COP, as shown in Fig. 6. The calculated performance curves fit the lowest drive voltage data fairly well and overpredict the 8.0 and 10.7 V<sub>rms</sub> performance. Note, that the %Carnot COP increases steeply from the no-load temperature to approach values around 20% at coldtip temperatures above 150 K. This is excellent performance. The %Carnot COP is seen to increase with drive level, reflecting the specific power improvement at higher drive voltages as noted in Fig. 4.

The thermal performance described above is sensitive to a number of other factors such as heatsink temperature, drive frequency, and cold-finger conduction. This data is provided in detail in [1], a short summary of these sensitivities is provided here. Increasing the heatsink temperature from 0°C to 20°C causes the isotherms pictured in Fig. 4 to shift to the left by 10 K. As a result, decreasing the heatsink temperature decreases the input power required to refrigerate a particular coldtip load at a particular coldtip temperature. Variation of the cooler drive frequency demonstrated that the 60 Hz design frequency provided the best thermal performance. Measurements of the cold-finger conduction showed that it increases with decreasing coldtip temperature to -1.6 watts at 100 K. This is a high parasitic loss when compared to a typical 80K cryocooler with 200 to 500 mW of parasitic loss. Some performance benefits could be derived from a smaller diameter and longer coldfinger.

**1. Load Curve Concavity.** The load curves for the 140K cooler demonstrate an unusual upward concavity (see Fig. 5). This behavior can be attributed to idealized performance where it is assumed that the heat transfer between the gas and the outside surface of the coldtip is perfect. Under these conditions it is relatively easy to show [3] that the lift and the cycle power are proportional as follows:

$$\begin{aligned} \text{Lift} &\propto \alpha_p X_p X_d \sin \phi \\ P_{\text{cycle}} &\propto \alpha_T X_p X_d \sin \phi \end{aligned}$$

where  $X_p$  and  $X_d$  represent the piston and displacer strokes,  $\alpha_p$  and  $\alpha_T$  represent the pressure and thermal coupling between the piston and displacer, and  $\phi$  represents the phase angle between the displacer and piston. By combining these two expressions, the lift can be expressed as:

$$\text{Lift} \propto \left( \frac{\alpha_p}{\alpha_T} \right) * P_{\text{cycle}}$$

For an isothermal cycle, the ratio  $\alpha_p/\alpha_T$  can be expressed in terms of temperatures and area ratios [3] to yield:

$$\begin{aligned} \text{Lift} &\propto \frac{\left(1 - \frac{A_k}{A}\right)}{\left(\frac{T_h}{T_c} + \frac{A_k}{A} - 1\right)} * P_{\text{cycle}} \\ \text{or: Lift} &\propto \frac{\frac{T_c}{T_h} \left(1 - \frac{A_k}{A}\right)}{\left(1 - \frac{T_c}{T_h} \left(1 - \frac{A_k}{A}\right)\right)} * P_{\text{cycle}} \end{aligned}$$

where  $A_k$  and  $A$  represent the displacer rod area and the displacer area, and  $T_h$  and  $T_c$  represent the heatsink and coldtip temperatures respectively. Now, since:

$$\frac{T_c}{T_h} \left(1 - \frac{A_k}{A}\right) < 1$$

the lift can be expressed in a Taylor series:

$$\text{Lift} \propto \frac{T_c}{T_h} \left(1 - \frac{A_k}{A}\right) \left[ 1 + \frac{T_c}{T_h} \left(1 - \frac{A_k}{A}\right) + \left(\frac{T_c}{T_h}\right)^2 \left(1 - \frac{A_k}{A}\right)^2 + \dots \right] * P_{\text{cycle}}$$

where higher order terms rapidly become insignificant, even for  $T_c$  approaching  $T_h$ . If  $A_k/A = 0.5$  the Taylor series approximation is good up to a coldtip temperature of about 210 K at a heatsink

temperature of 300 K. For this cooler, the ratio  $A_R/A$  is less than 0.1.

It is easily seen from the final lift expression that the lift increases with increasing cold tip temperature  $T_c$  if the cycle power is held constant. In the measurements discussed above and plotted in Fig. 4 the input power was nearly constant over each load curve, however, the power factor was not constant, and the heat transfer in the coldtip is certainly not infinite. All these factors will modify the load curve. In this particular case, the motor efficiency improves at warmer temperatures which actually increases the order of the curve. Furthermore, when the lift is plotted against the coldtip temperature for a constant input voltage, see Fig. 5, the motor efficiency and its mechanical tuning arc such that the piston amplitudes arc generally higher for warmer temperatures which again increases the lift.

There is only one factor that acts to reduce the order of the curve and that is finite heat transfer. As the lift increases with warmer temperatures, the coldtip heat exchanger becomes overwhelmed by the high heat flux and the temperature differential between the cold gas and the outside wall of the coldtip increases. Since the cycle operates between the gas temperatures, the lift will eventually asymptote as the heat load is increased. This problem is much more severe in smaller cryocoolers where often no formal heat exchanger exists at the coldtip. The 140K cooler, however, does have a formal coldtip heat exchanger that is designed to transfer at least 35 watts with a small temperature differential. Therefore, this machine exhibits lift behavior that is closer to that expected from ideal theory rather than the typical asymptotic curve that is generally seen.

## VIBRATION

Measurements of the cooler vibration were conducted in the JPL cryocooler vibration characterization facility using a special-purpose six-degree-of-freedom dynamometer. This dynamometer has a frequency range from 10 to 500 Hz and a force sensitivity from 0.005 N (0.001 lb) to 445 N (100 lbs) full scale. During operation, the generated forces ( $F_x, F_y$ , and  $F_z$ ), and moment ( $M_z$ ) about the cooler's  $z$  axis, arc simultaneously recorded in real time using a spectrum analyzer. Fig. 7 shows that the measured forces and moment increase with increasing drive voltage as expected. The magnitude of the  $F_z$  fundamental increases from 17 lbs to 38 lbs when the drive voltage is increased from 5.3 Vrms to 10.7 Vrms. The future addition of an active counterbalancer needs to be considered for applications requiring low vibration levels.

This cryocooler has no instrumentation to provide information about the compressor or displacer stroke. However, an estimate of the piston stroke can be made from the measured force levels at a particular drive voltage to see whether they arc comparable to the strokes determined by the linearized model (see discussion above). The stroke is calculated according to the following equation:

$$x_p \approx \frac{F_z}{m(2\pi f)^2}$$

where  $F_z$  represents the fundamental force component determined from dynamometer measurements,  $m$  represents the moving mass of the piston, and  $f$  represents the fundamental frequency. It is assumed that the displacer's contribution to this peak force is negligible due to its small mass. In this case, the mass of the piston is 255 gm and the drive frequency is 60 Hz. The comparison between the calculated strokes and the strokes determined from the fundamental force harmonic is shown in Fig. 8. Note that the calculated compressor stroke is sensitive to the heatsink temperature; the higher the heatsink temperature, the lower the piston stroke. The dynamometer measurement recorded at 10.7 Vrms is at thermal equilibrium but the dynamometer

measurements at 8.0 V<sub>rms</sub> and 5.3 V<sub>rms</sub> are not at thermal equilibrium. The heatsink temperature of the cooler while mounted on the dynamometer was higher than 20°C. Despite the fact that the heatsink temperature was higher in these measurements than in the thermal performance calculated from the model, it appears that the calculated stroke lengths are certainly reasonable when compared to these few known data points.

Coldtip vibratory displacement amplitudes were obtained by measuring the coldtip acceleration using a three-axis accelerometer and then dividing each acceleration harmonic by the square of its harmonic frequency in radians/see, i.e. the displacement (x) at frequency (f) is computed as:

$$x = \frac{a}{(2\pi f)^2}$$

where (a) represents the measured acceleration at the same frequency. Coldtip displacements in the x, y, and z directions for the coldtip of the Sunpower 140K cooler are shown in Fig. 9. The z-axis is directed toward the coldtip along the axis of the cooler. Note, that the axial displacements are larger than the lateral ones for the fundamental and second harmonic. Also, the x displacements are smaller than the y displacements at all harmonics. At the fundamental frequency the x displacements are an order of magnitude smaller than the y displacements. There is no obvious asymmetry within the cooler that would indicate a reason for such a difference.

## RESONANCE

The compressor and displacer resonant characteristics are measured by driving the compressor with a constant amplitude sinusoidal current that is swept through a range of frequencies surrounding the nominal cooler drive frequency. Constant amplitude sinusoidal current corresponds approximately to constant amplitude sinusoidal force applied to the permanent-magnet motor. Because the Sunpower cooler lacks the instrumentation required to measure piston or displacer amplitude and phase, the test technique involved running the cooler on the force dynamometer and measuring the cooler's force transmissibility. The cooler's resonance parameters are determined by least-squares fitting to the measured transmissibility [5]. To provide data for both ambient launch environments and operational environments, measurements were made at both ambient and cryogenic temperatures. This is important because the stiffness of the working gas drops with coldtip temperature and the cooler's resonance characteristics change accordingly.

Fig. 10 presents the force transmissibility (F<sub>z</sub>) measured at ambient temperature for a range of drive currents. Note that the natural resonance of the piston only occurs for drive currents of 2.4 amps and greater; this is because the gas bearing system for the piston does not become operational until after static friction forces are overcome and the piston develops a finite stroke. This type of seal may offer some advantageous resistance to launch excitation. Note that the resonance is very close to 60 Hz. Despite the presence of the passive displacer, no double peaks were found in the ambient temperature data. Curve fits were computed for the 2.8-amp and the 3.0-amp data; the resulting parameter values are presented in Table 1. The effective spring stiffness and critical damping coefficient were then calculated from these parameters using the moving mass provided by Sunpower.

At cryogenic coldtip temperatures, the resonance curves, shown in Fig. 11, took on a distinctly different shape. The resonance from the displacer has become apparent, creating a double peaked resonance. The dual peaks are found near 54 Hz and 65 Hz. In general, the resonant frequency of a cryocooler compressor decreases at cryogenic temperatures; therefore, it appears that the compressor has reached a resonant frequency of 54 Hz. The peak at 65 Hz can therefore be

attributed to the displacer resonance. Notice that the generated force levels are lower than those obtained for the ambient coldtip temperatures; this implies a significant increase in damping at cryogenic temperatures as is usual for Stirling cryocoolers. As at ambient temperature, currents above 2.4 Amps were required to achieve normal piston motion.

Table 1. Summary of drive resonance parameters for Sunpower 140K cooler.

	<u>COL. DTIP TEMPERATURE</u>	
	<u>Ambient</u>	<u>Cryogenic</u>
<b>COMPRESSOR</b>		
Natural Frequency, Hz	59	54
Damping Ratio, $C/C_c$	0.05	*
Moving Mass, kg	0.255	0.255
Spring Stiffness, N/mm	<b>35.0</b>	<b>29.4</b>
Critical Damp. Coef. ( $C_c$ ), N-s/m	189	173
<b>DISPLACER</b>		
Natural Frequency, Hz	59	65
Damping Ratio, $C/C_c$	*	*
Moving Mass, kg	0.033	0.033
Spring Stiffness, N/mm	4.5	5.5
Critical Damp. Coef. ( $C_c$ ), N-s/m	24.5	26.9

\* = Not available

## EMI

The EMI measurements were made with the cooler placed in a steel RF-shielded room and grounded to a copper-laminated table. During the testing the drive electronics were placed in an adjacent area outside the shielded room with connecting cabling fed through a bulkhead in the wall. The cabling is sheathed in aluminum foil and grounded to the copper table top to minimize any contributing radiation. The cooler was operated at 10.0 Vrms to create maximum-level emissions. The AC magnetic field emissions were measured at a 7-cm distance from the cooler, corresponding to MIL-STD 461 C:RE 01, and at a 1-m distance, corresponding to a modified MIL-STD 461 C:RE 04 test method (see Fig. 12). The electric field was measured at a distance of 1 m from the cooler axis. Ambient background measurements were also made for comparison.

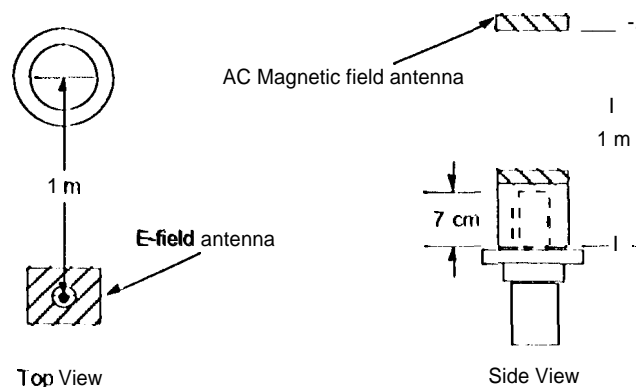


Figure 12 Measurement locations for electric field and AC-magnetic fields.

The results from the 7-cm measurement location are shown in Fig. 13. The measurements are presented in units of dB-pT, i.e., decibels relative to 1 picoTesla. The reference line represents the allowable level specified in 1<1301. Note, that the first two harmonics of the cooler drive frequency exceed the specification limit. This performance is typical for space cryocoolers of similar input power. Note that the EMI was measured while powering the cooler with linear-amplifier laboratory power supplies; therefore, the measurements do not contain high-frequency EMI that is typical of a high-efficiency PWM-type power converter that would normally be used in a spacecraft application. At a distance of 1 m, the AC magnetic field was about 10 dB greater than the background, and the electric field was nearly indistinguishable from the background levels.

The DC magnetic field was measured in three planes (x, y, and z) at a distance of approximately 1 m. For these measurements the cooler was disconnected from the drive electronics and was mounted inside a set of DC coils that generate a magnetic field to cancel the earth's magnetic field inside the test volume. The magnitude of the DC magnetic field was found to be 55 nT at a distance of 1 m.

## CONCLUSIONS

The results presented above summarize the measured performance of the Sunpower 140K cryocooler. Comparison of the thermal performance data with the calculated results yielded very good agreement. In general, the 140K cooler exhibited remarkable overall performance; this is even more impressive considering it resulted from a modification of an existing cooler rather than a formal ground-up design process. The characterization accentuated the cooler's shortcomings particularly in the area motor efficiency and parasitic heat load. A new higher powered linear motor from Sunpower, rated at 91% efficiency, has been built into a ground-up designed cryocooler that is capable of achieving lower temperatures. In addition, a smaller diameter and longer coldfinger has been utilized on the new cooler to reduce the parasitic heat load. A performance curve for this cooler, calculated from the linear theory using the physical characteristics of that machine, is shown in Fig.14. The calculated lift is 4 watts at 77K.

## ACKNOWLEDGEMENT

The experimental work described in this paper was carried out by the Jet Propulsion Laboratory, California Institute of Technology, for the Air Force Phillips Laboratory, Albuquerque, New Mexico and the Los Angeles Air Force Base, Space and Missiles Systems Center. The work was sponsored by the Strategic Defense Initiative Organization under a contract with the National Aeronautics and Space Administration. Particular credit is due F. Jetter, who produced the graphs presented herein, S. Leland, who provided assistance and support with many of the test setups, and P. Narvacz, who carried out the electromagnetic compatibility measurements.

References herein to the Sunpower cooler, or to any specific commercial product, process, or service by tradename, trademark, manufacturer, or otherwise, does not constitute or imply its endorsement by the United States Government or the Jet Propulsion Laboratory, California Institute of Technology.

## REFERENCES

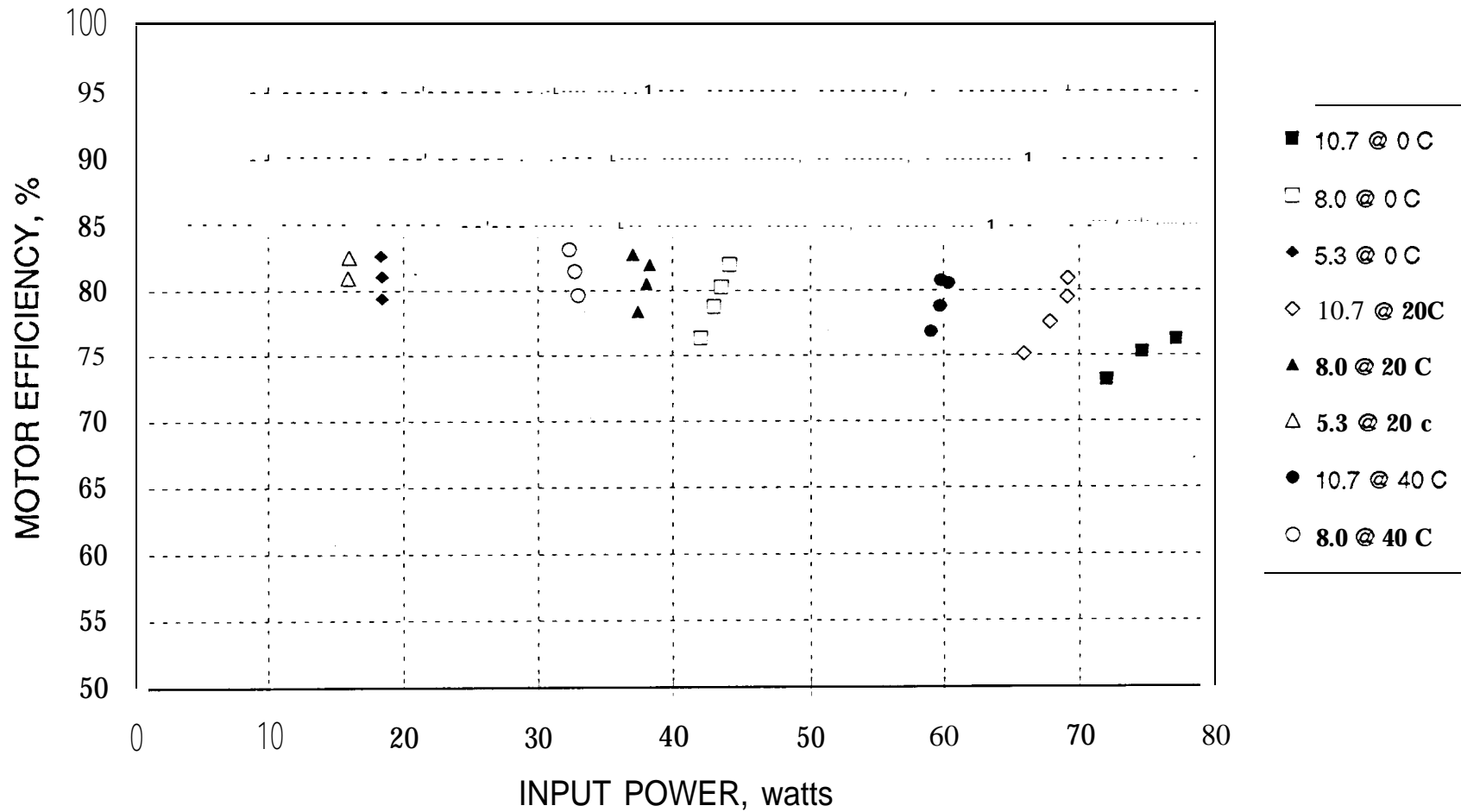
1. G. P. Smedley, D. L. Johnson, and R.G. Ross, Jr., Sunpower 140K Cryocooler: Performance Characterization, JPL Document D-11085, July 1993.
2. Redlich, R.W. and Berchowitz, D. M., "Linear Dynamics of Free-Piston Stirling Engines", Proc Instn Mech Engrs, vol. 199, no. A3 (1985), pp. 203-213.
3. Berchowitz, D.M., "Free-Piston Stirling Coolers", International Refrigeration Conference - Energy Efficiency and New Refrigerants, Purdue University, July 1992, pp. ???-???
4. de Jong, A. K., "A Small Free-Piston Stirling Refrigerator", 14th IECEC, Boston, paper 799245, August 1979, pp. 1136-1141.
5. Ross, R. G., Jr., et al., "Cryocooler Resonance Characterization". Proceedings of the 1993 Space Cryogenics Workshop, San Jose, California, July 20-21, 1993.

## FIGURE CAPTIONS

- 1 External appearance of Sunpower 140K cooler.
- 2 Measured %motor efficiency at various drive voltages and heatsink temperatures.
- 3 Measured magnetic loss.
- 4 Multivariable plot of measured and calculated thermal performance at 20C.
- 5 Measured and calculated load curves of thermal performance at 20C.
- 6 Measured and calculated %Carnot COP at 20C.
- 7 Vibrational forces at several drive voltages.
- 8 Compressor stroke determined from dynamometer measurements compared with the calculated stroke.
- 9 Measured coldtip displacements vs frequency.
- 10 Force resonance measured at ambient coldtip temperature.
- 11 Force resonance measured at cryogenic coldtip temperature.
- 12 Measurement locations for electric field and AC-magnetic fields.
- 13 AC Magnetic field measured at 7cm from cooler.
- 14 Calculated load curve for 77K cooler.



# SUNPOWER 140K COOLER SENSITIVITY OF MOTOR EFFICIENCY TO INPUT POWER



~~Alternator~~ Alternator Magnetic Loss

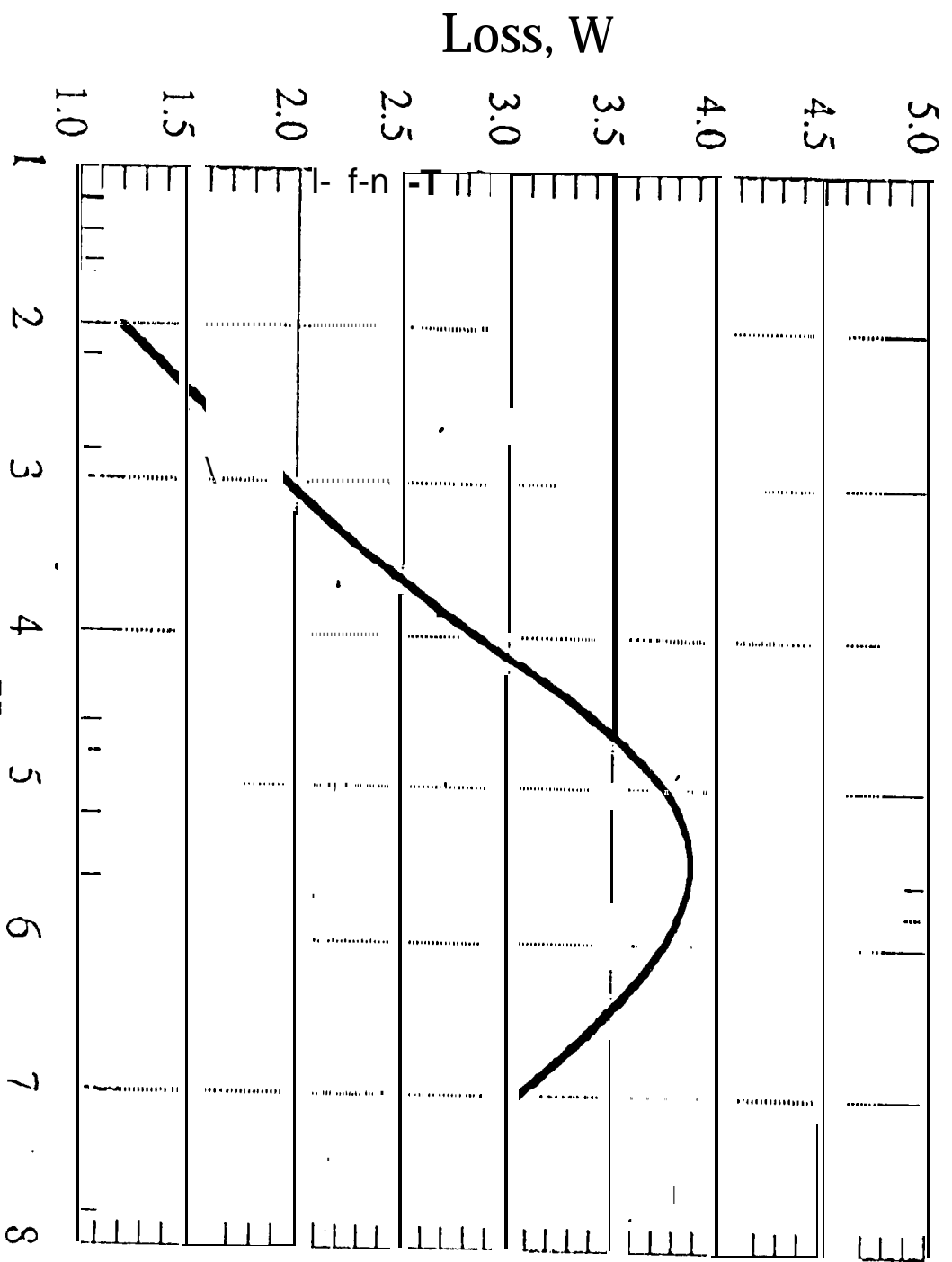


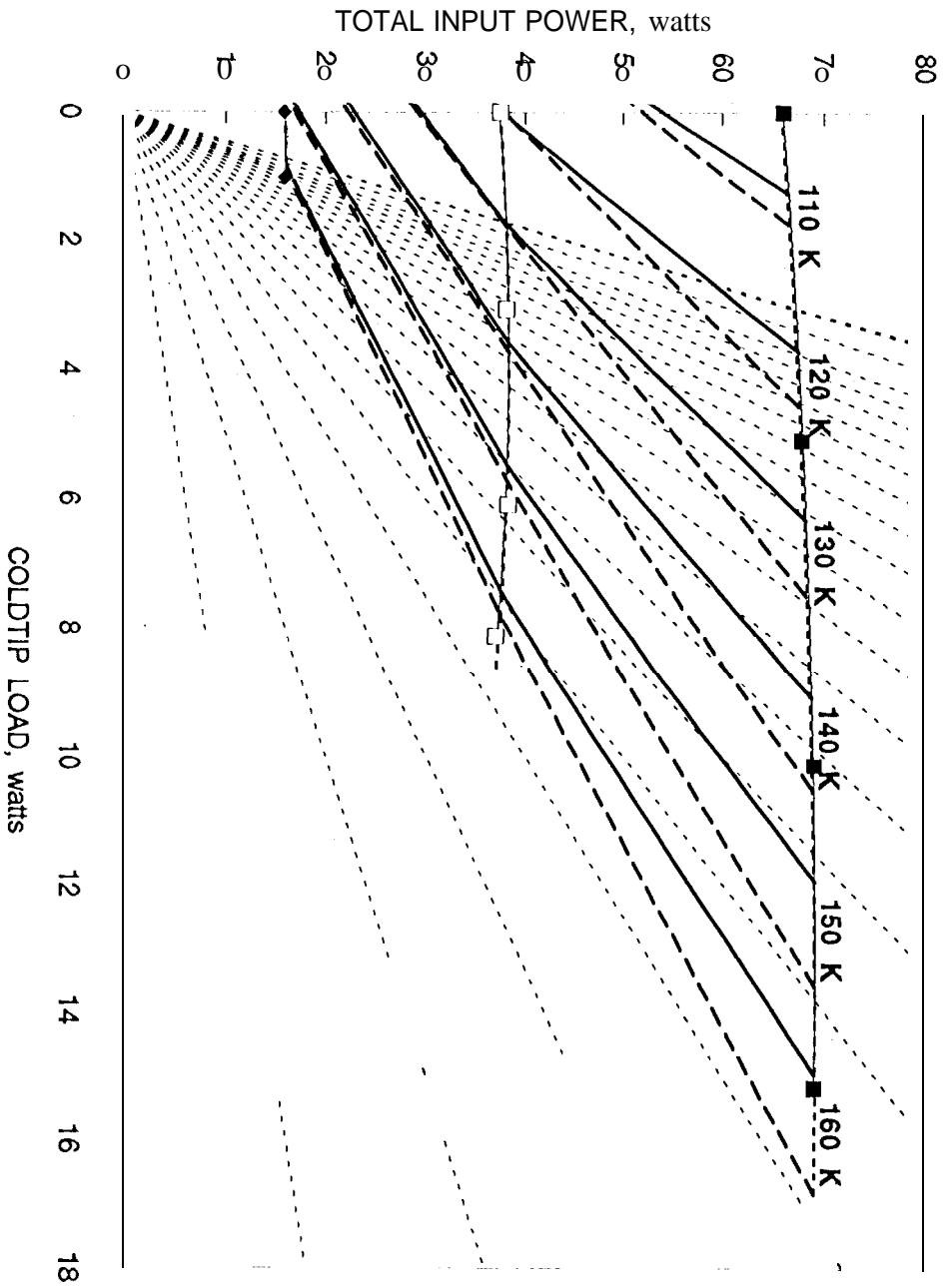
Fig. 3

Fig (Mag loss)

\*\*\*END\*\*\*

# SUNPOWER 140K COOLER SENSITIVITY OF THERMAL PERFORMANCE TO DRIVE VOLTAGE

HEAT SINK TEMPERATURE = 20C



G. Smedley

Fig. 4

3/24/94

[Sunpap\_Rs.xlw]"Ross"-plotd

**SUNPOWER 140K COOLER  
SENSITIVITY OF THERMAL PERFORMANCE TO DRIVE VOLTAGE**

HEATSINK TEMP = 20 C

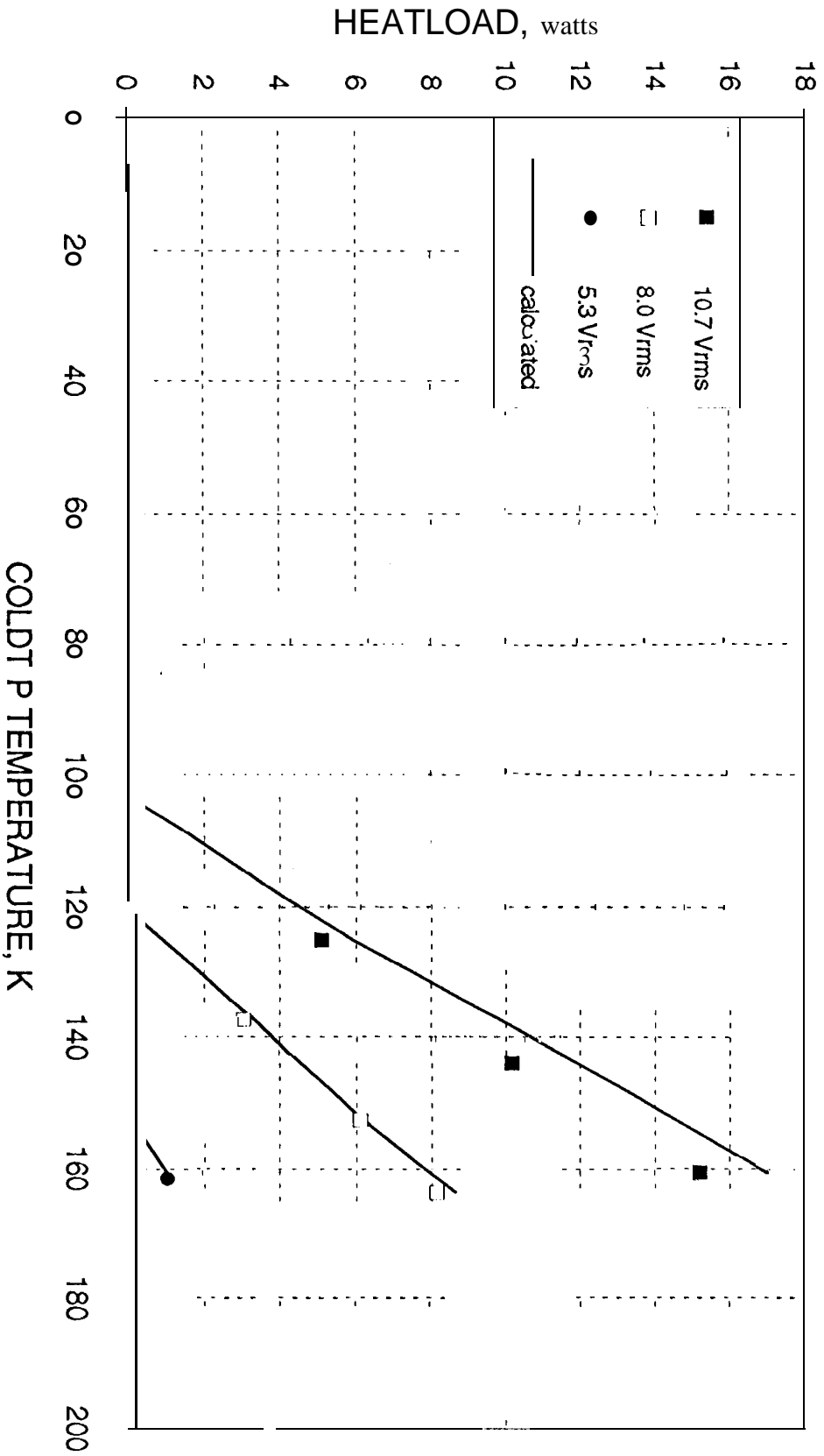
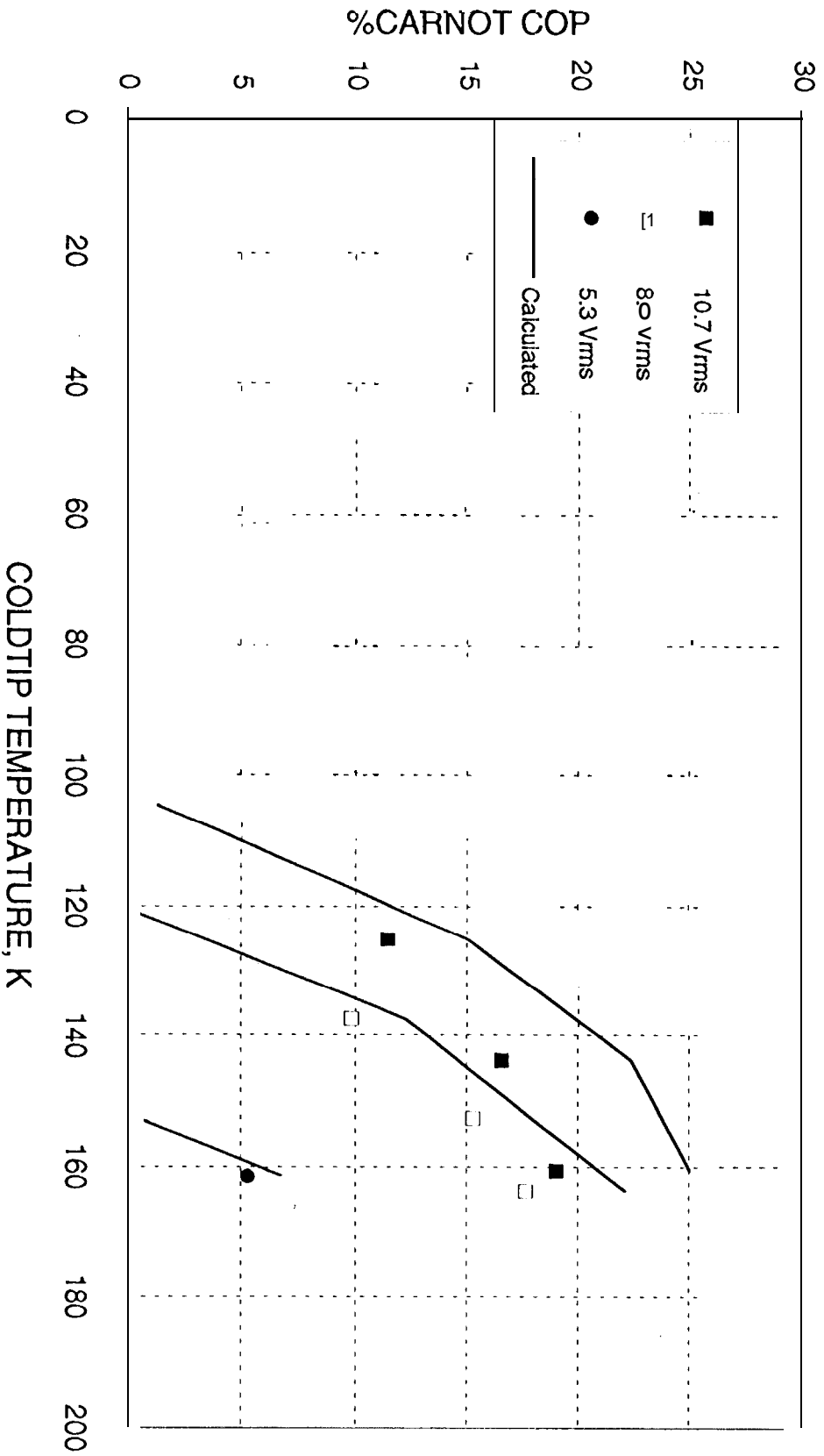


*Fig. 5*

**SUNPOWER 140K COOLER**  
**SENSITIVITY OF %CARNOT COP TO DRIVE VOLTAGE**  
 HEAT SINK TEMPERATURE = 20 C



G. Smedley

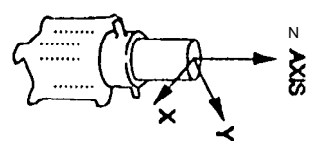
Fig. 6

4/12/94

[Sunpapr.xlw]%COP\_Tct

# SUNPOWER 140K COOLER VIBRATION AT VARIOUS INPUT VOLTAGES

COLDTIP AT CRYOGENIC TEMPERATURE  
FUNDAMENTAL FREQUENCY: 60 HZ  
NO PASSIVE BALANCER



DRIVE VOLTAGE	
	5.3 Vrms
	8.0 Vrms
	10.7 Vrms

9-L

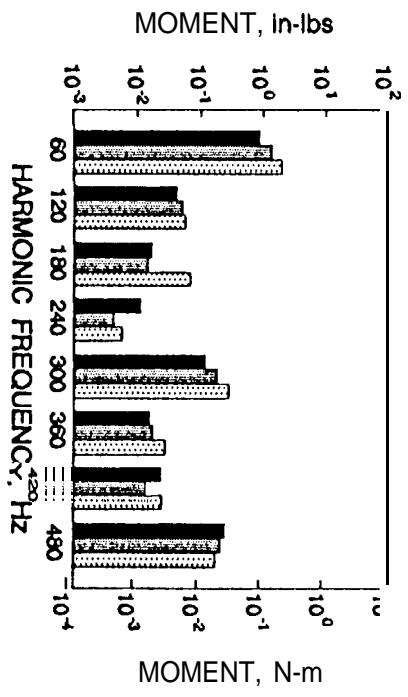
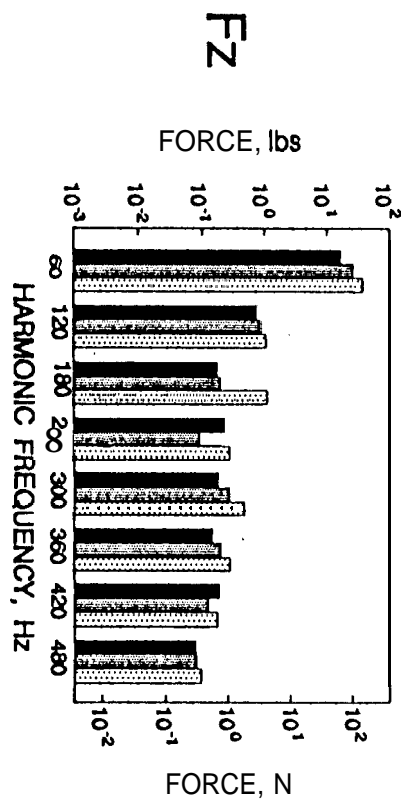
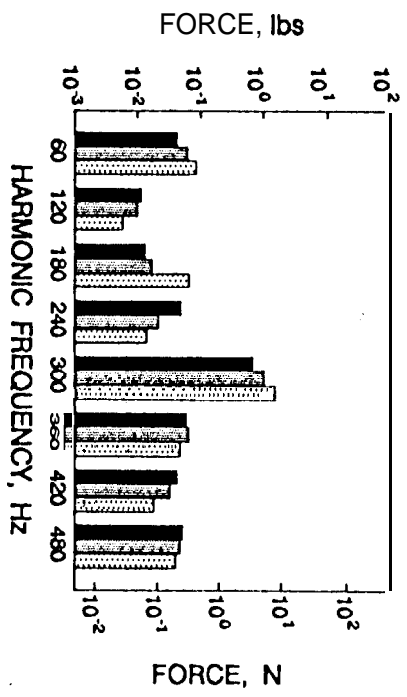
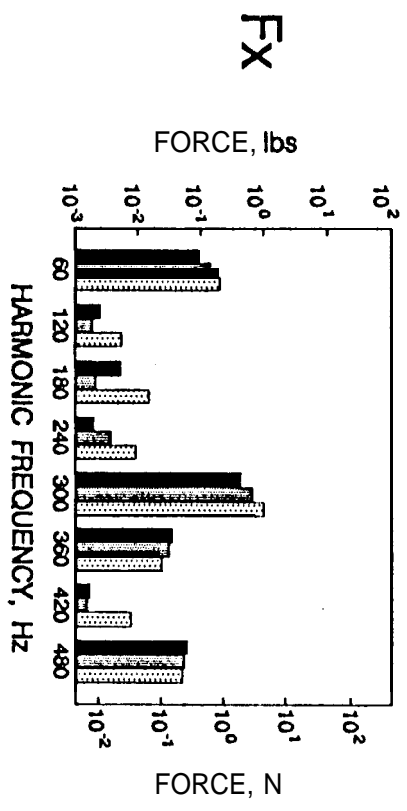
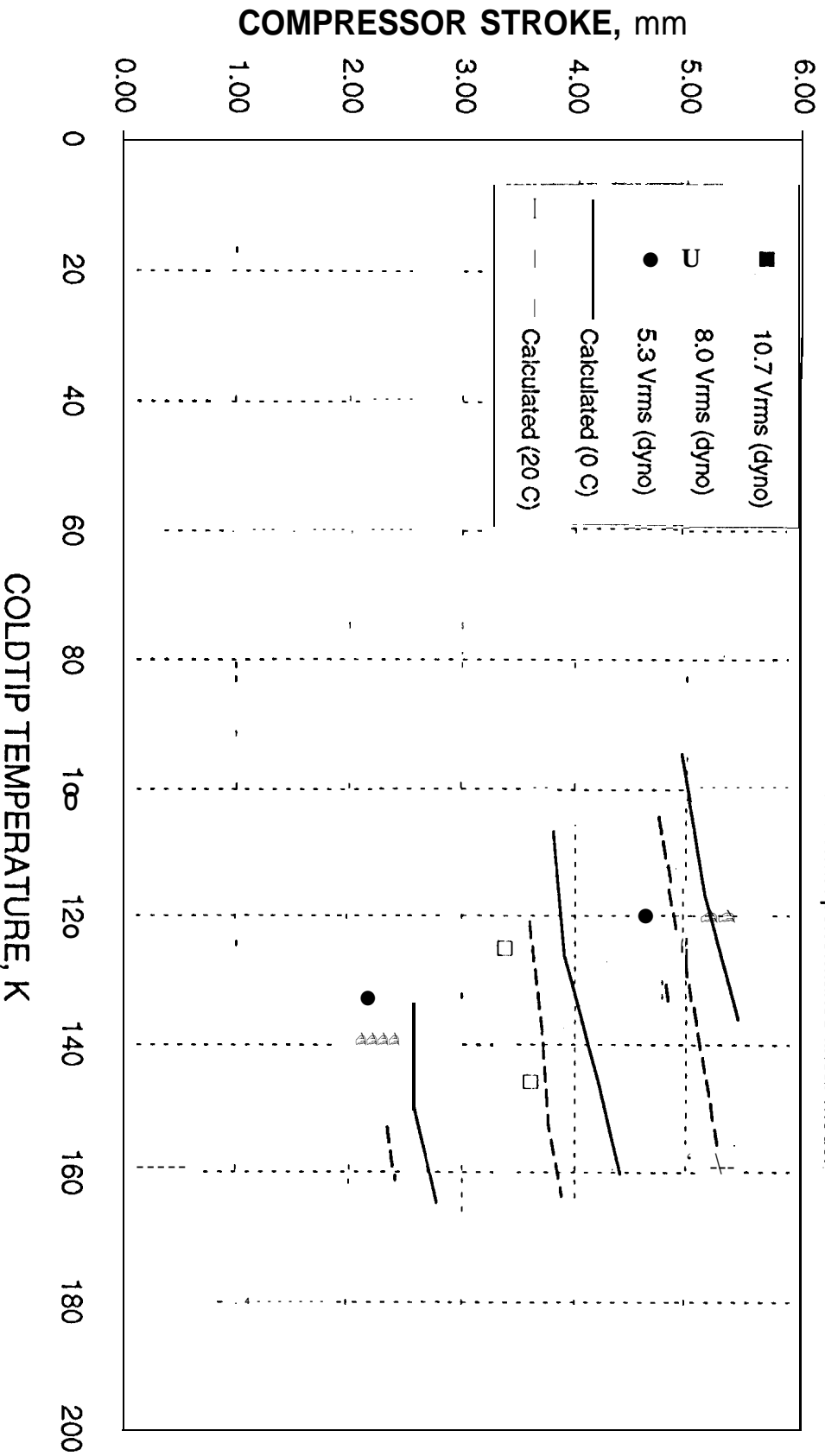


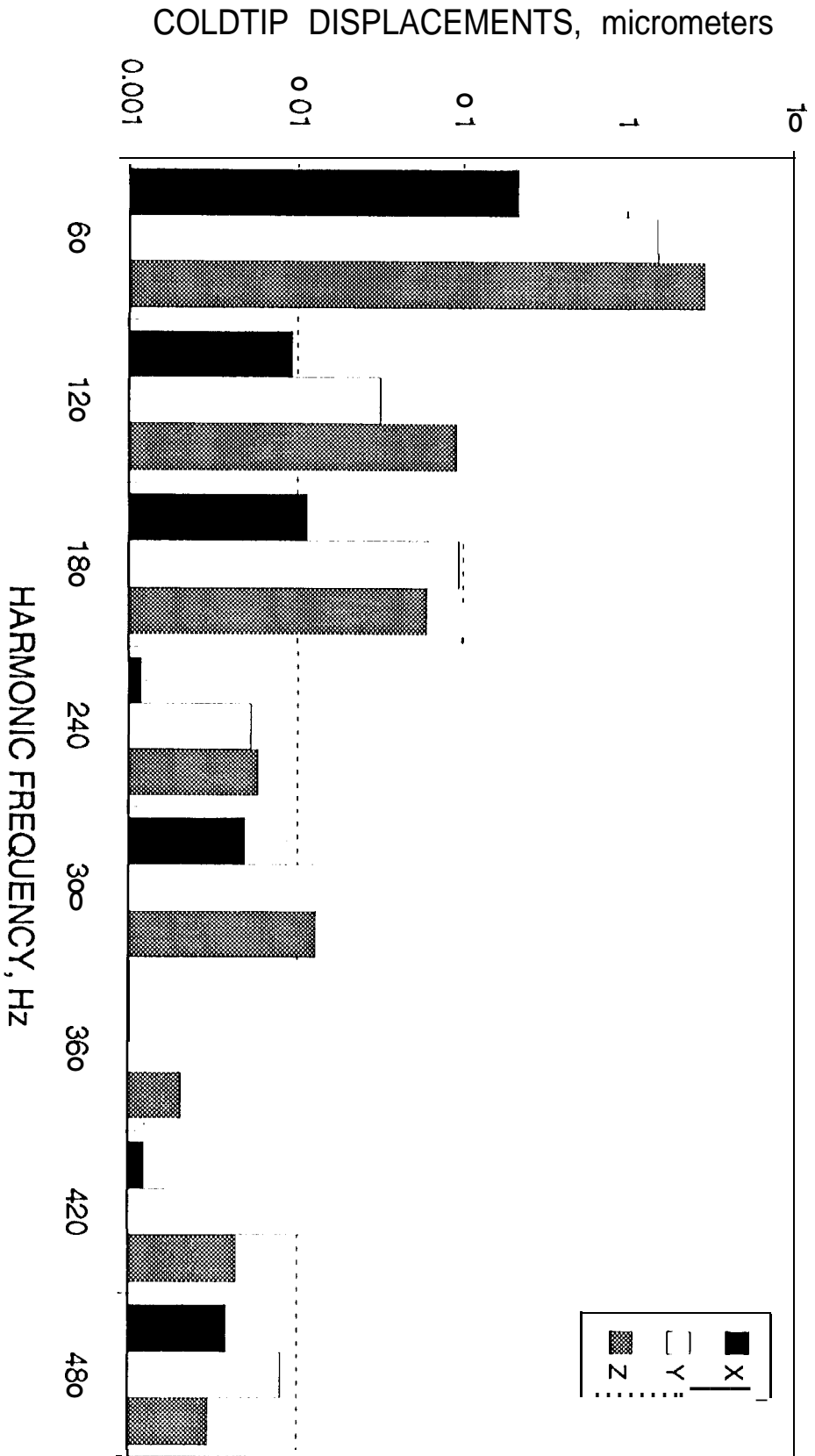
Fig. 7

# SUNPOWER 140K COOLER SENSITIVITY OF COMPRESSOR STROKE TO COLDTIP TEMPERATURE

(dyno) => Estimated from Fz dyno measurements (not at equilibrium)  
 Calculated => Results from thermal performance linear model



# SUNPOWER 140K COOLER COLDTIP DISPLACEMENT SPECTRA



G. ed

Fig. 9

3/25/94

W

# SUNPOWER 140K COOLER SWEEP-SINE FORCE RESONANCE AMBIENT TEMPERATURE

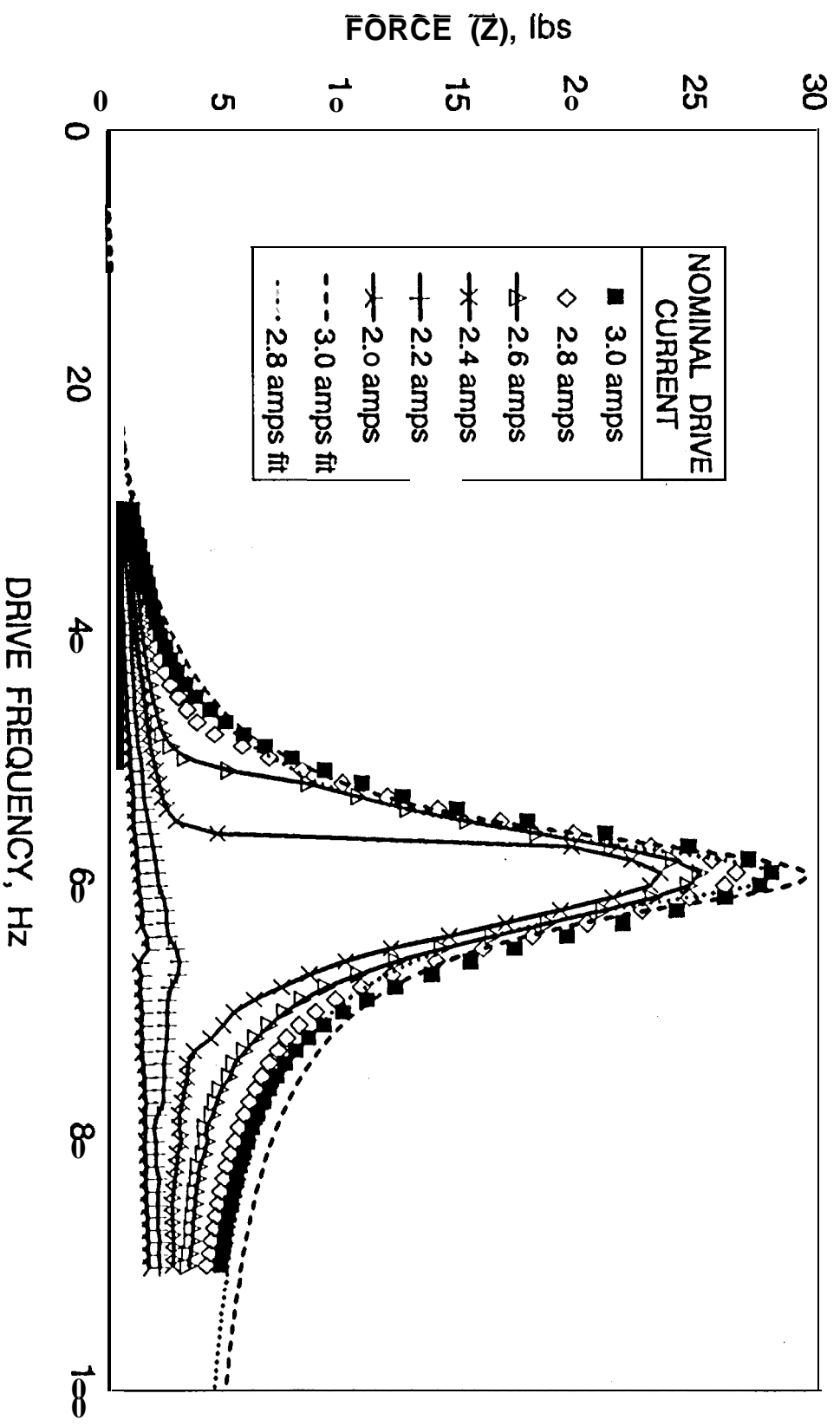
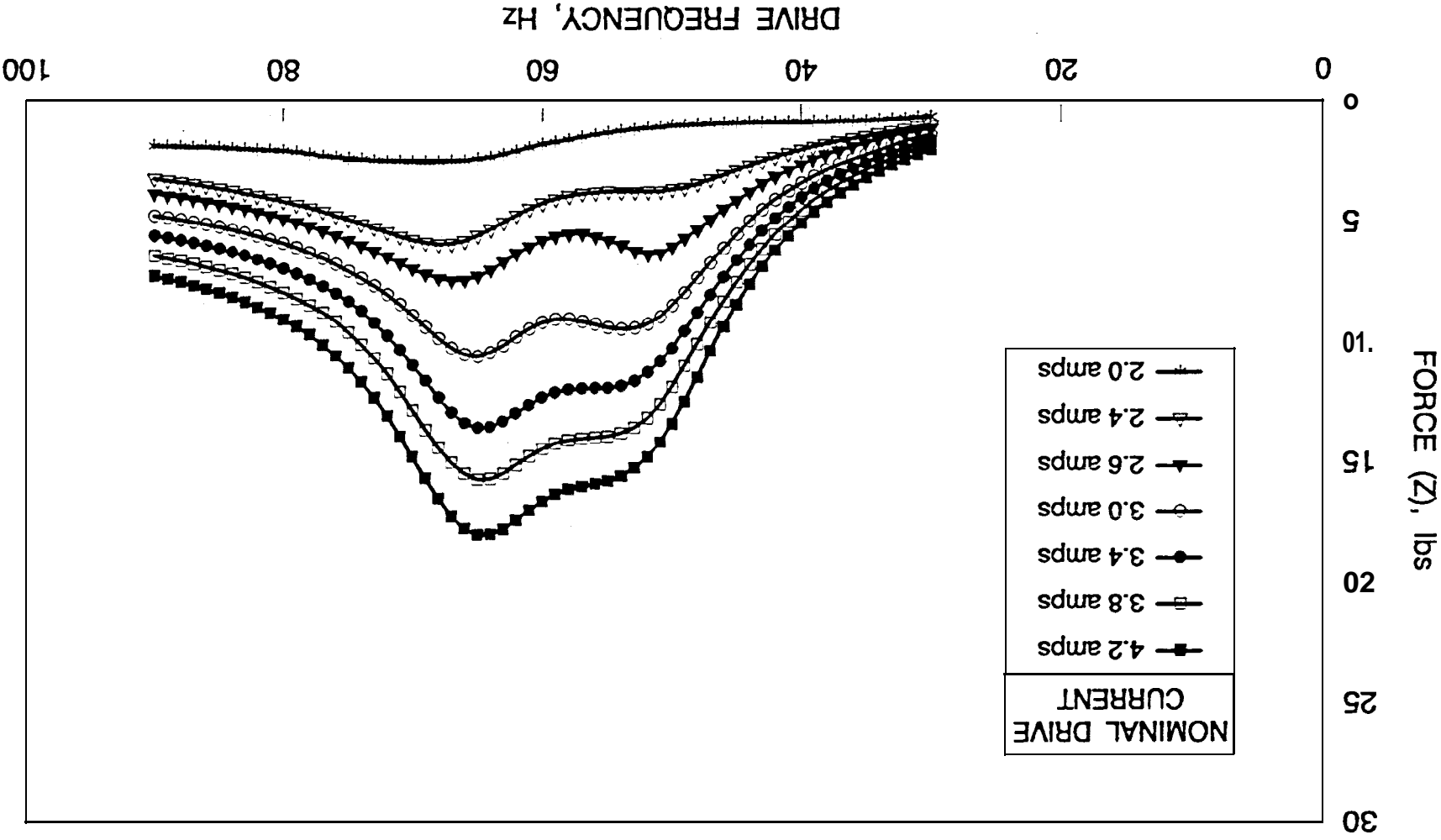


Fig. 10

# SUNPOWER 140K COOLER SWEEP-SINE FORCE RESONANCE CRYOGENIC TEMPERATURE



8-9

SUNFBTY.WK3

Fig 11

SUN\_26

# SUNPOWER 140K COOLER AC MAGNETIC FIELD EMISSIONS MIL-STD 461C RE01

ANTENNA 7 cm FROM HEAT SINK PLATE; DRIVE VOLTAGE = 10.0 Vrms

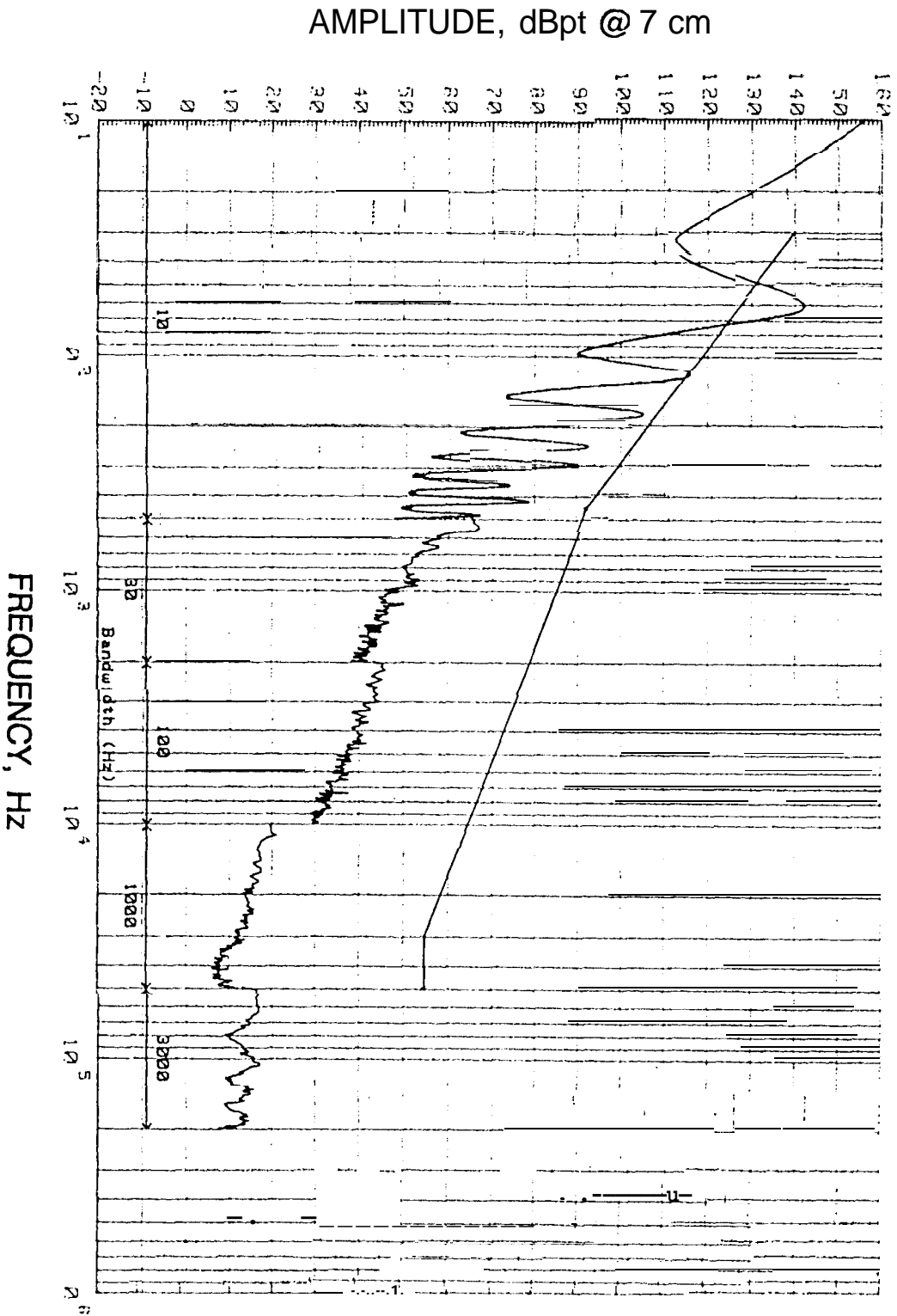
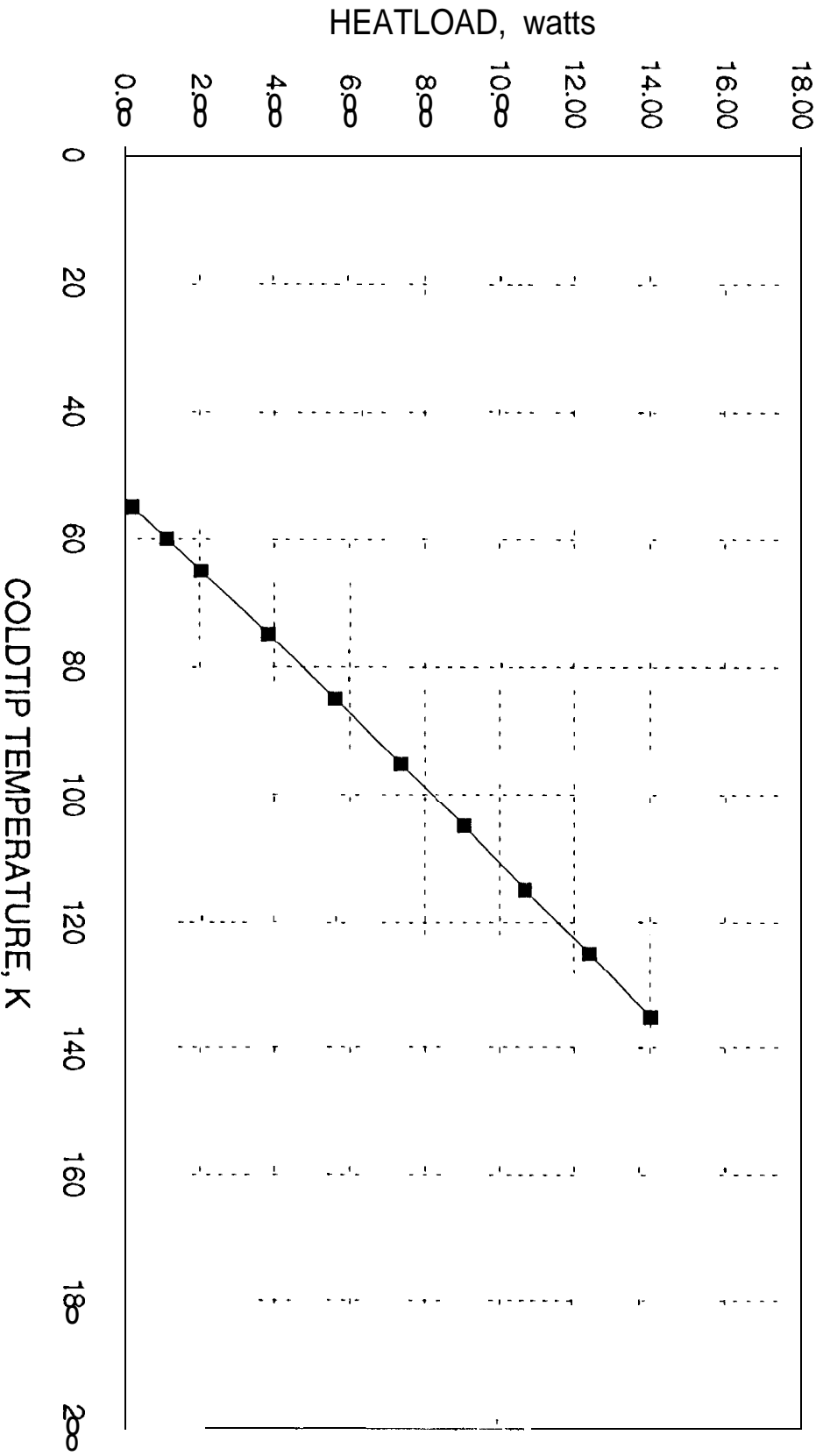


Fig. 13

# SUNPOWER 77K COOLER CALCULATED THERMAL PERFORMANCE

COMPRESSOR STROKE = 5.2 mm; HEATSINK TEMPERATURE = 320 K



G. Smedley  
*Fig. 14*

4/18/94

[Sunpaper.xlw]77Kcurve